

Article

Progressive Deformation Patterns from an Accretionary Prism (Helminthoid Flysch, Ligurian Alps, Italy)

Pierre Mueller ¹, Matteo Maino ^{1,2,*}  and Silvio Seno ¹

¹ Dipartimento di Scienze della Terra e dell'Ambiente, Università di Pavia, 27100 Pavia, Italy; pierre.mueller01@universitadipavia.it (P.M.); silvio.seno@unipv.it (S.S.)

² Istituto di Geoscienze e Georisorse, CNR, via Ferrata 1, 27100 Pavia, Italy

* Correspondence: matteo.maino@unipv.it

Received: 16 December 2019; Accepted: 9 January 2020; Published: 11 January 2020



Abstract: This paper reports the results of a field-based structural investigation of a well-exposed paleo-accretionary prism, which experienced complex deformation in a low-grade metamorphic setting. Field analyses focused on the description of structural fabrics, with the main emphasis upon parameters like the orientation, style and kinematics of foliations, folds and shear zones. We address the research to the south-westernmost part of the Alpine chain, the Ligurian Alps, where, despite their origin as turbidite sequences deposited into the closing Alpine Tethys Ocean, the Helminthoid Flysch Nappes are presently distributed in the outer part of the chain, above the foreland. The new dataset highlights different deformation patterns related to the different spatial distribution of the flysch units. This regional-scale partitioning of strain is hence associated with progressive deformation within a two-stage geodynamic evolution. Correlations among the different orogenic domains allow the proposal of a kinematic model that describes the motion of the Helminthoid Flysch from the inner to the outer part of the orogen, encompassing the shift from subduction- to collision-related Alpine geodynamic phases.

Keywords: orogenic wedge; subduction flysch; oceanic closure and continent collision; deformation phases; progressive deformation

1. Introduction

The evolution of a collisional orogen entails multiple and overlapping deformation stages that reflect the physical variations during the three-dimensional spatiotemporal evolution of the incorporated rock units. Such variations derive from the effect of variable tectonic stresses affecting rocks which are heterogeneous in terms of their composition and inherited structure, and that deform under variable temperature and lithostatic pressure conditions. The resulting complex pattern is classically simplified and grouped into deformation and/or metamorphic phases characteristic of one or more tectonic domains. Each deformation phase is generally accompanied by one generation of foliation or schistosity representative of the deformational regime and the metamorphic conditions [1–3]. Changes in the orientation and/or strength of the tectonic forces, as well as in the temperature and pressure conditions, generate penetrative structures that display different orientations and shapes. In field-based studies, the determination of multiple overlapping fabrics represents the key factor to unravel the deformational history of an orogenic domain [1]. However, even within a single tectonic domain the deformation patterns may be strongly heterogeneous in response to local lithological variations or inherited geometry. Hence, the regional-scale correlation of structural fabrics among different outcrops may be difficult. Moreover, similar deformation patterns may result from different mechanisms that involve one or multiple deformation phases.

Local or regional structures may be the result of distinct deformation phases, progressive deformation, or a combination of the two [4]. Such complexities are often underestimated, whilst the number of the locally observed foliations are typically uncritically appraised, and expanded to large tectonic domains. Consequently, robust regional interpretations may become challenging. Therefore, to reduce uncertainties, field analyses should precisely indicate how and where each structural fabric occurs. Subsequently, a critical evaluation (i.e., a comparison with the other outcrops) should be performed, with the main emphasis being put upon the determination of the temporal and spatial variations of the deformation and the generating mechanisms [1,2,4].

In this paper, we present a field-based, structural analysis of the uppermost portion of the paleo-accretionary wedge preserved in the Ligurian Alps. The Ligurian Alps are the southernmost portion of the Alpine chain. They preserve a complete stratigraphic record of the European and oceanic (Alpine Tethys) paleogeographic domains (Figure 1; [5–12]). In particular, the turbiditic covers of the ophiolite sequences, namely the Helminthoid Flysch units, are well exposed in the outermost part (SW) of the chain, thrust directly onto the foreland (Figure 2)—despite the fact that they were detached from their innermost position (NE) in close vicinity to the subduction trench. Although the absence of high-grade metamorphism is clear evidence of thin-skinned thrusting, the kinematic of the translation and emplacement of the Helminthoid Flysch nappes is still poorly understood [8,10]. They show heterogeneous structural fabrics and both longitudinal and traversal geometric variations, and therewith prevent a trivial kinematic interpretation. The data presented in this study allow the linkage of the fabric and geometric heterogeneities to regional variations which can be integrated into an evolutionary path that incorporates their variations in space and time.

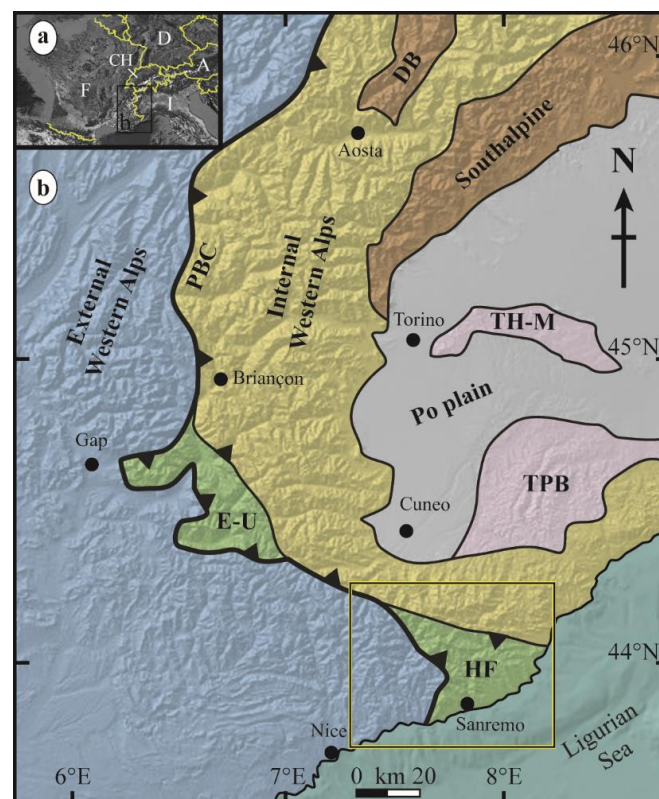


Figure 1. (a) Location of the study area. (b) Tectonic sketch of the Western and Ligurian Alps [12]. Tectonic units are grouped into Internal (Piedmont, Piedmont–Ligurian and Briançonnais) and External (Provençal–Dauphinois, Helvetic and External Massifs) domains. The yellow box shows the location of the Helminthoid Flysch nappes (HF) above the Penninic Basal Contact (PBT). DB: Dent Blanche nappe (Austroalpine domain); E-U: Embrunais-Ubaye nappes; TH-M: Torino hill and Monferrato high; TPB: Tertiary Piedmont Basin.

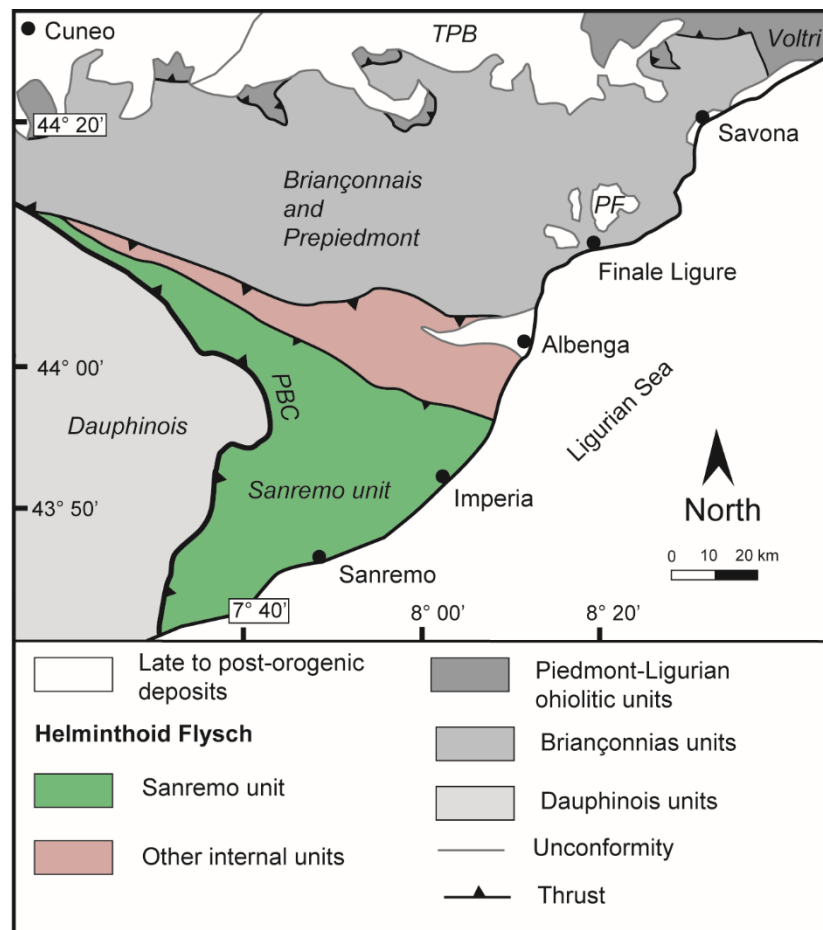


Figure 2. Tectonic setting of the Ligurian Alps [6,8,12], showing the main paleogeographic domains (Piedmont–Ligurian, Prepiedmont, Briançonnais and Dauphinois). The Helminthoid Flysch nappes rest above the Briançonnais–Dauphinois boundary through the Penninic Basal Contact (PBC). PF: Miocene-age Pietra di Finale deposits; Voltri indicates the Voltri Massif of the Piedmont–Ligurian oceanic basement.

2. Geological Setting

The Helminthoid Flysch nappes represent the structurally topmost units of the Ligurian segment of the Western Alps (Figure 1; [6,8,10]). The Alpine edifice is formed by imbricated tectonic units, which are interpreted to be derived from the four main different paleogeographic domains: (1) the Dauphinois, i.e., the proximal European margin; (2) and (3) the Briançonnais and Prepiedmont, the outer and inner parts of the distal margin, respectively; and (4) the Piedmont–Ligurian, representing the neo-Tethyan oceanic basin (Figure 2; [5–7,9,12]). The ensemble of the allochthonous domains 2, 3 and 4 is termed the Penninic domain.

The convergence between the Adriatic and European plates since the Late Cretaceous encompassed the closure of the interposed Piedmont–Ligurian Ocean and the subduction–collision process during Eocene–Oligocene times [5–7]. The oceanic basement, together with most of the Briançonnais terrane, experienced HP metamorphic conditions during subduction [13–16], whereas the Pre-Piedmont units and the oceanic sedimentary covers (i.e., the Helminthoid Flysch nappes) were obducted, recording only epi- to anchi-metamorphism [12,17–20]. The present-day structure of the Ligurian Alps comprises a tectonic pile that mainly preserves a geometric order that reflects the paleogeographic provenance of the unit. The terranes derived from the oceanic basement–Piedmont–Ligurian presently occupy a structurally higher and more inward (E or NE) position, whereas the Prepiedmont, Briançonnais and

Dauphinois domains are progressively situated at a lower and more outwards (W or SW) position (Figure 2).

The Dauphinois domain represents the autochthonous foreland onto which the other Penninic units thrust along the so-called Penninic Basal Contact, here represented by the basal thrust of the Helminthoid Flysch nappes [8,20–23]. However, striking to the structural position of the Piedmont–Ligurian basement, the detached Helminthoid Flysch units are presently located in the outermost part of the chain where they directly rest upon the Dauphinois domain, a structural position that highlights an independent travel path during wedge translation.

Due to the subduction–collision processes, each tectonic unit experienced variable deformation and metamorphism, which are traditionally classified into three major ductile phases (D1–3) that developed in Eocene–Early Oligocene times [6,8]. Each phase is associated with a foliation (S1–3) and correlated with an orogeny-scale geodynamic stage. A first phase (D1) is characterized by foreland-vergent (SW in present-day coordinates) isoclinal or sub-isoclinal folding, nappe formation and thrusting [8,10,21–24]. A second phase (D2) is interpreted to have produced hinterland-vergent (NE) folding and back thrusting [6,8,10,21,25]. It developed under decreasing metamorphic conditions during exhumation [25]. Instead, open chevron and kink folds are generally associated with a third ductile phase (D3), possibly generating asymmetric dome-and-basin interference patterns [8,10,21,25]. Brittle deformation became dominant since the upper Early Oligocene, when transtensional/transpressional fault systems, which are associated with the rifting of the Liguro–Provençal basin and the Corsica–Sardinia drifting, induced the $\sim 50^\circ$ Neogene rotation of the Ligurian and internal SW Alps [26–31]. The final emplacement of the Helminthoid Flysch nappes is constrained between 34 and 28 Ma by means of zircon (U-Th)/He absolute dating of the basal thrust [20].

The Helminthoid Flysch complex includes five tectonic elements. These are, from top to bottom: the Sanremo, Moglio–Testico, Borghetto, Colla Domenica–Leverone and Albenga units (Figure 3). The first four units consist of: 1) Lower–Upper Cretaceous “basal complexes” made up of thin-bedded and very fine-grained turbidites. They often display chaotic texture defined by enveloping ophiolitic blocks as part of a sedimentary mélangé. The basal complexes are overlain by 2) Upper Cretaceous–Early Eocene sand-rich- or calcareous turbidite systems [32–41]. Observable thickness of the units ranges between 500 and 2000 m. The basal complexes are interpreted as representing abyssal plain sediments. They are juxtaposed by thick-bedded siliciclastic or calcareous turbidites interpreted to be deposited in a trench environment [36,37]. Detrital zircon U-Pb data [38,39] indicate a similar source for both formations, compatible with the magmatic and metamorphic pulses recorded in the Variscan basements of the paleo-European margin [42–46]. By contrast, the Albenga unit is made up of calcareous turbidites that directly superimpose Late Jurassic radiolarites. They have been interpreted to represent a part of the detached cover of the underlying Prepiedmont Arnasco–Castelbianco unit, which is the innermost nappe that features a complete Triassic–Eocene succession. The Arnasco–Castelbianco unit marks the transition between the oceanic domain (Piedmont–Ligurian) and the European distal margin [9,19,47].

With regard to the metamorphic grade, each flyschoid unit shows upwards-decreasing conditions, even in the epizone to anchizone conditions [19]. Specifically, several paleothermal indicator analyses performed on the Sanremo unit indicate a peak temperature of up to 200 °C, while hotter conditions were attained in the cataclasites of the basal thrust [20].

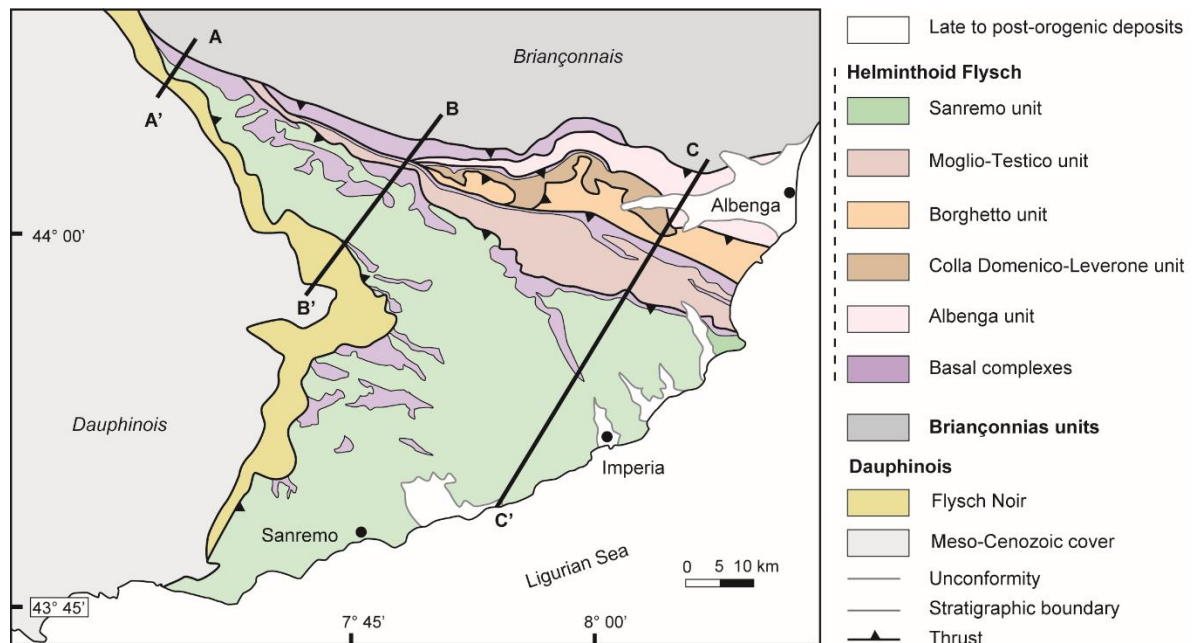


Figure 3. Simplified geological map of the Helminthoid Flysch nappes, from [32,37,40,41]. Location of cross-sections are shown.

3. Methods

The study is based on structural investigations of three key geological cross-sections along SW–NE transects (see Figure 3), which represent the inferred main tectonic transport direction. These sections have been selected, since they represent the main geometrical and deformation features of the studied units. We performed field analyses on the regional topographic maps of the Liguria and Piedmont Regions, at a 1:10,000 scale. The structural data and observations have been transferred on a Geographic Information System (GIS)-based storage (QGis). Sections and figures were built or modified using Adobe Illustrator. Stereonet plots were computed using Stereonet3D [48].

4. Results

The structure of the Helminthoid Flysch nappes is described along three geological cross-sections running perpendicular to the main thrust and fold axes mapped in the field:

4.1. Cross-Section A-A'

Section A-A' crosses the northern sector occupied by the Helminthoid Flysch complex (Figures 3 and 4), which is here exclusively represented by the uppermost tectonic element, the Sanremo unit. It consists of mainly NE-dipping beds (Figure 4) of reddish or grayish pelites to fine-grained arenites (San Bartolomeo Formation, which is part of the basal complex), which are overlain by partly heteropic quartz–feldspatic arkoses (Bordighera Sandstones) and calcareous turbidites (Sanremo Formation) [34,37,49]. They are intensively folded in south-west-verging, Recumbent, subisoclinal folds with axes plunging toward the SE or NW (Figure 5a,b). These are associated with a discrete axial plane cleavage (Figure 5b) and several generations of fractures filled by calcite veins. Deformation in the pelitic basal complex shows disharmonic folding with axes plunging mainly toward the SE. The Sanremo unit is separated from the underlying Dauphinois domain by the thick thrust zone of the Penninic Basal Thrust [10,20], which is characterized by a wide damage zone (up to 1 km) developed both in the hanging wall (Sanremo unit) and the footwall, here represented by the Late Eocene–Early Oligocene siliciclastic turbidites of the Flysch Noir [40,41,50]. Minor fault zones subparallel to the

main thrust displaying an en-echelon array of veins also occur. Moving towards NE, the Sanremo unit shows a steep and overturned thrust contact with the Briançonnais Cretaceous calcschists (Figure 4).

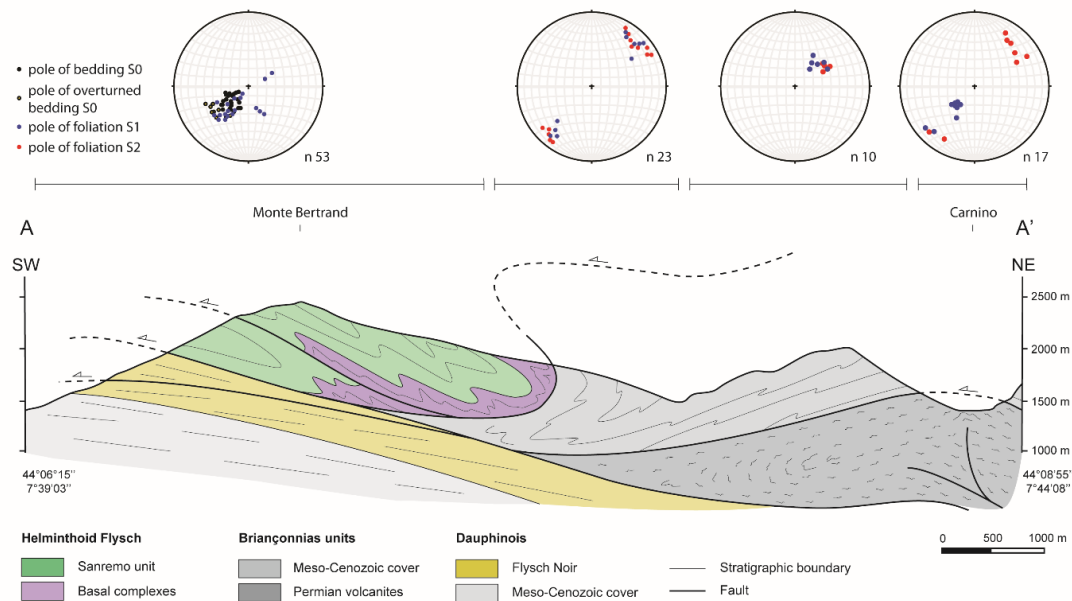


Figure 4. Cross-section A-A'. See Figure 3 for the map location. Lower hemisphere, equal area stereonet of representative foliation data. The section has been divided into four sectors that are internally homogeneous.

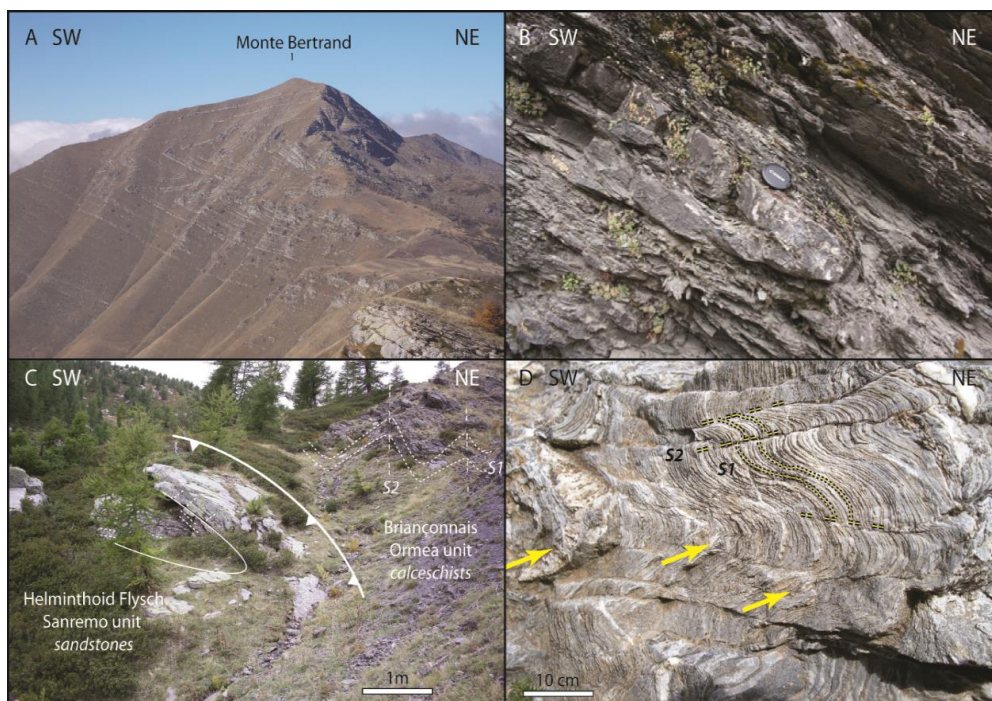


Figure 5. Deformation features from cross-section A-A'. Sub-isoclinal folding of the carbonate turbidites (A) and pelite basal complex (B) in the Sanremo unit. Rocks from the Sanremo unit show a single foliation (B,C), whereas the Briançonnais calcschists show two overlapping foliations with different orientations (C,D).

This contact shows a clear inversion of the geometric relationships between the Helminthoid Flysch and the Briançonnais (Ormea unit; [8,51–53]), and marks an abrupt change of the structural fabric. In fact, despite both the basal pelites and the sandstones of the Sanremo unit showing only one single foliation, the Briançonnais rocks locally display two overlapping foliations (S1 and S2; Figure 5c,d). Two distinct penetrative foliations are reported from all sectors of the Ligurian Briançonnais [6,8,10,24,51–53]. In the examined area, S2 appears as a crenulation of a previous foliation associated with the folding of the stratigraphic layering (Figure 5d). In the Briançonnais sector, attitudes of both S1 and S2 dip towards the SW or the NE, while the Sanremo unit displays a single (S1), less steep NE dipping (Figure 4).

Overall, the mapped stratigraphic boundaries, the fabrics measurements, and the mesoscale folds depict a main recumbent SW-verging fold, which has been reshaped by an upright fold that caused an apparent double vergence of the structures, as well as the overturning of the thrust between the Sanremo unit and the Briançonnais (Figure 4).

4.2. Cross-Section B-B'

Moving towards the SE, section B-B' resumes the structure of the central part of the Helminthoid Flysch nappes (Figures 3 and 6). The outer (SW) part of the section is similar to the previous one, showing the thrust of the Sanremo unit above the Flysch Noir of the Dauphinois domain (see [24] for a complete description). In addition, the deformation features are almost identical, with intense kink to tight folding associated with one axial plane foliation in the calcareous and siliciclastic turbidites of the Sanremo unit (Figure 7a). The pelites of the basal complex again display constant SW-verging disharmonic folding (Figure 7b). Northeastward, the thrust between the Sanremo unit and the Moglio–Testico unit is still overturned [35]. The turbidites of the Moglio–Testico unit consist of a dominantly overturned, thin-bedded pelitic-arenaceous sequence, characterized by intense SW-plunging folding, strongly crenulated and sheared, but maintaining the same SW-ward kinematic (Figure 7c). However, a second, overprinting foliation is manifested by the SW dipping thin shear zone with reversal movement (top-to-NE), locally cross-cutting the earlier SW-vergent folds (Figure 7c). Moving towards NE, extensive basal complex outcrops, exhibiting chaotic features and characterized by abundant ophiolitic olistostromes, occur. Because of the lack of an overlying turbiditic sequence, its attribution to a unit is difficult, although they appear to resemble the deformational features of the Moglio–Testico sediments. Finally, calcschists and limestones of the Briançonnais Ormea unit show well-developed minor isoclinal folds associated with a normal limb of a mega SW-verging recumbent fold (Figure 7d), which is locally sheared and/or refolded by steeply dipping reverse faults or upright folds associated with a second foliation (S2). In the sector occupied by the Moglio–Testico and the Briançonnais rocks, S1 and S2 have similar attitudes, either NE or SW dipping, whereas the Sanremo unit still shows a single NE dipping foliation (Figure 6).

Overall, the general interpretation of the cross-section B-B' shows: (i) a western sector characterized by a single foliation and a single tectonic transport towards SW, and (ii) a more complex, apparently double vergent (SW and NE), eastern sector, consisting of a main, south-dipping mega-fold that involves the Briançonnais and the internal flysch nappes.

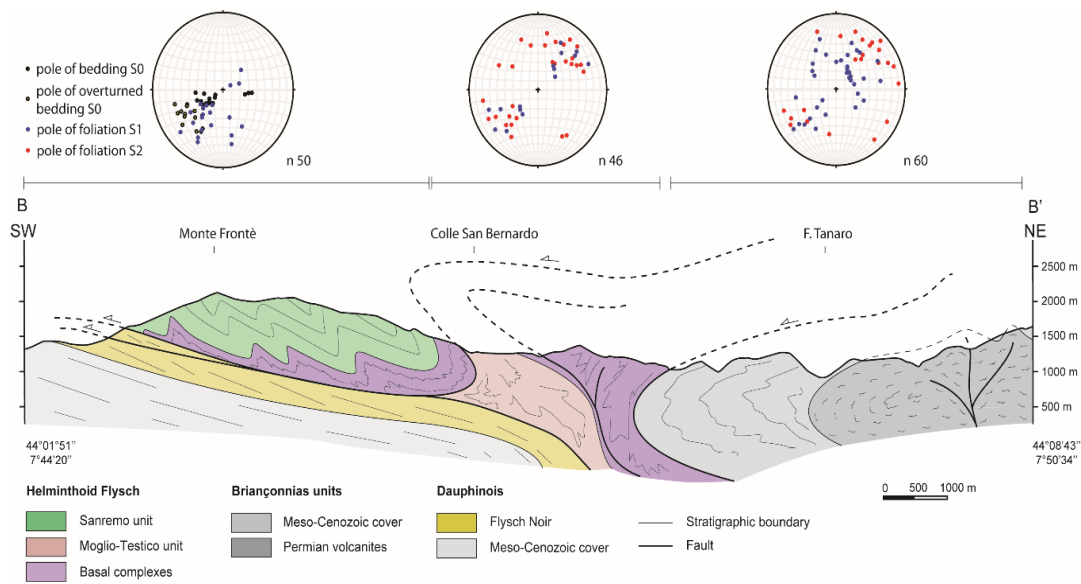


Figure 6. Cross-section B-B'. See Figure 3 for the map location. Lower hemisphere, equal area stereonet of representative foliation data. The section has been divided in three sectors internally homogeneous.

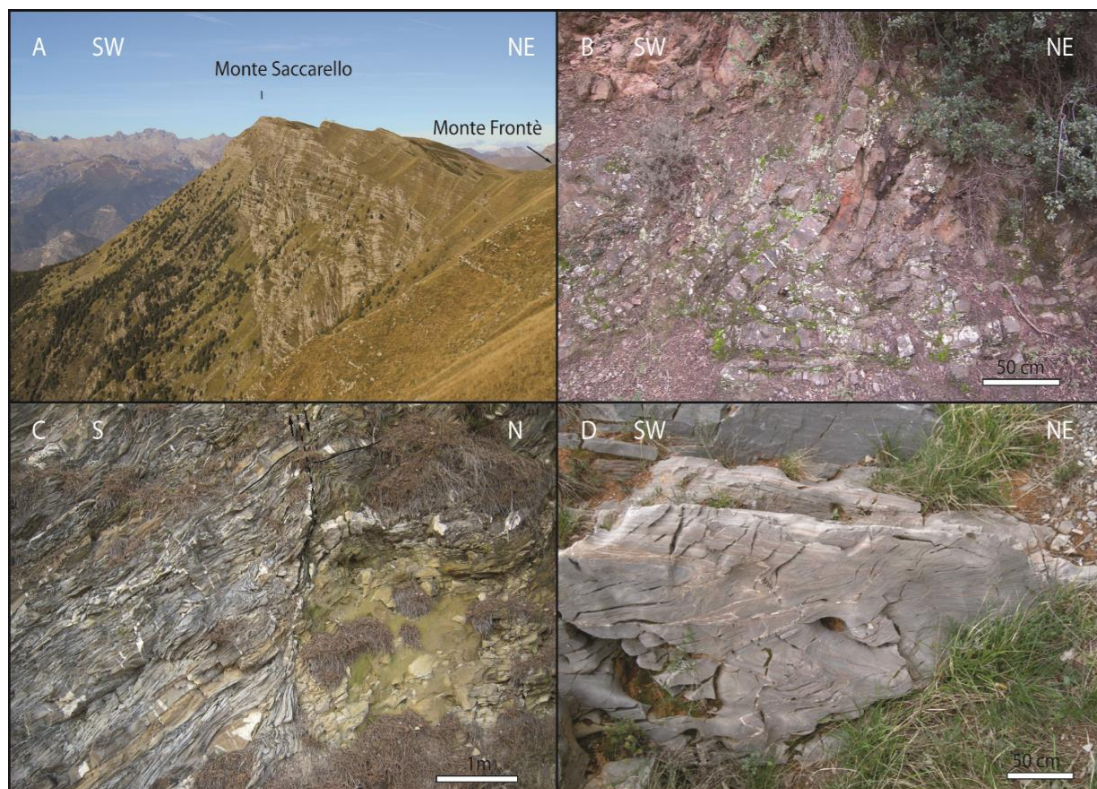


Figure 7. Deformation features from cross-section A-A'. Chevron folding of the calcareous San Remo Flysch turbidites (A) and disharmonic folding of the pelitic basal complex (B) of the Sanremo unit. Thin-bedded, mainly overturned, arenaceous-pelitic turbidites of the Moglio–Testico unit which show: (i) southwest dipping and verging isoclinal folding strongly crenulated and veined and (ii) high-angle, top-to-NE or -SW shear zones (C). SW-verging sub-isoclinal recumbent folds in the Briançonnais limestones (D).

4.3. Cross-Section C-C'

Cross-section C-C' runs close to the maximum map extension of the Helminthoid Flysch (Figure 3). It intersects all of the Helminthoid Flysch units, including, from NE to SW: the Albenga, Colla Domenica–Leverone, Borghetto, Moglio–Testico and Sanremo units (Figure 8). The frontal thrust cannot be seen here, as it occurs offshore. The Sanremo unit displays recumbent chevron folds, which dominantly affect the thick calcareous turbiditic strata (Figure 9a,b). These folds are always associated with one foliation, highlighted by a slaty cleavage in the fine pelites or marls, turning into a spaced disjunctive cleavage in the more competent limestones or calcareous sandstones (Figure 9c). The thrust surface that separates the Sanremo from the Moglio–Testico unit is generally steep, and in parts overturned, resulting in a local geometric inversion of the two nappes (Figure 9d; [54]). The more internal nappes (Albenga, Colla Domenica–Leverone, Borghetto and Moglio–Testico units) share a different deformation fabric. Here SW-verging and -plunging subisoclinal folds (Figure 9d) show abundant parasitic folds, crenulation, calcite-filled veining and synthetic shear zones (Figure 9e). These folds are often cut by high-angle reverse faults (with a mainly top-to-NE sense of shear), as those described in the section B-B' (Figure 9e–f). Overall, except for the Sanremo unit, all of the internal flysch units, as well as the neighboring Prepiedmont Arnasco–Castelbianco unit, are structured as SW-verging and south-plunging mega-folds (Figure 8; [55]). The latter presumably represents the original basement of the Albenga flysch, which was detached during the Alpine phases. The Arnasco–Castelbianco unit forms a km-scale, SW-dipping fold that shows a thin and delaminated normal limb, while the overturned limb is widely exposed (Figure 8; [55]). The general structure of the cross-section C-C' is quite similar to the sections A-A' and B-B'. S2 foliations are less developed, as also testified by minor evidence of the refolding of the main, southwest-dipping structure (Figure 8).

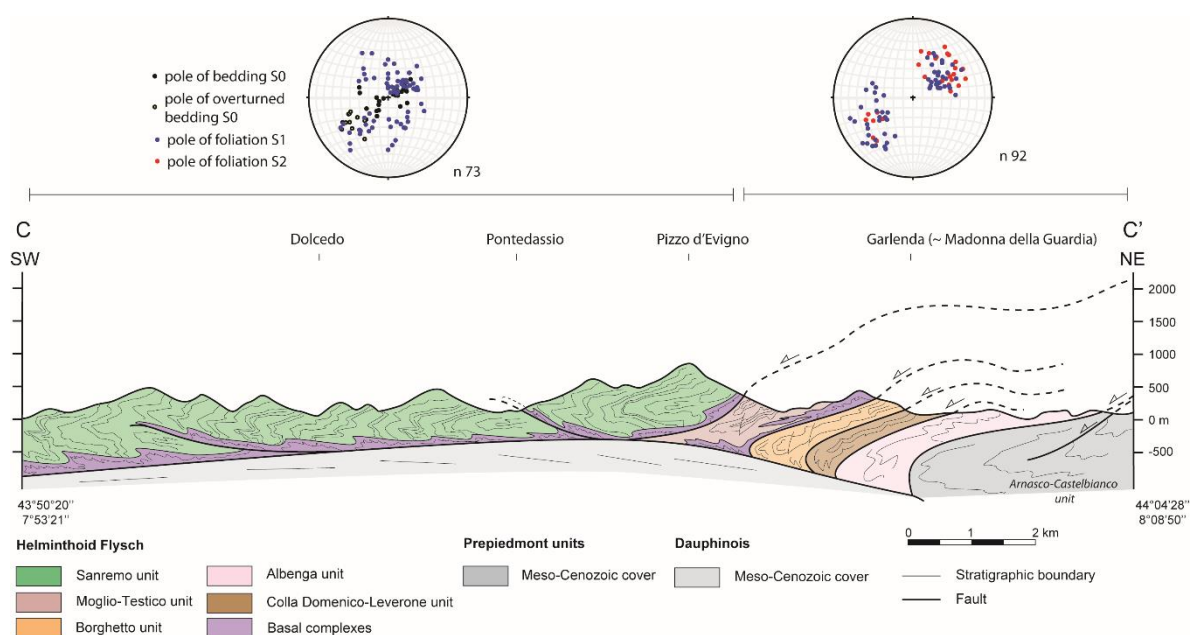


Figure 8. Cross-section C-C'. See Figure 3 for the map location. Lower hemisphere, equal area stereonets of representative foliation data. The section has been divided in two sectors internally homogeneous.

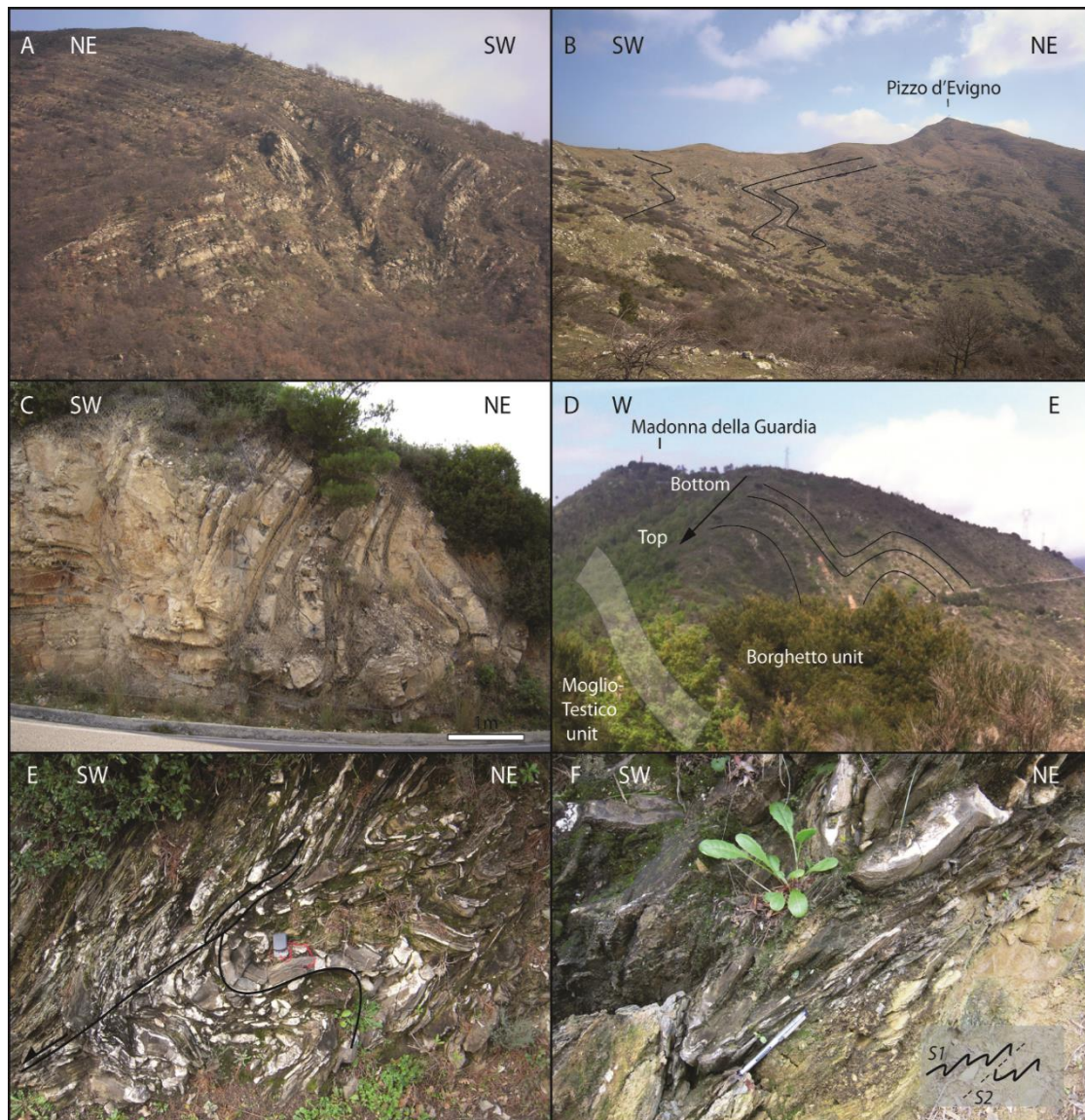


Figure 9. Deformation features from cross-section C-C'. Chevron folding of the carbonate turbidites in the Sanremo unit (A–C). The overturned geometry of the contact between the Borghetto and Moglio–Testico boundary (D). Foreland-dipping folds strongly crenulated and veined and associated synthetic shear zones (E). Top-to-NE brittle shear zones in the Moglio–Testico turbidites (F).

5. Discussion

5.1. Helminthoid Flysch Deformation Pattern

The structural dataset of the examined area allows researchers to evaluate the robustness of the correlations among subareas, facilitating considerations about the different fabric orientation, style and kinematics.

Bedding attitudes (S0) in the Sanremo unit display mostly uniform, NE-dipping folds characterized by steeper overturned limbs associated with a single foliation (S1) throughout the studied area. This foliation is defined by an axial plane cleavage that varies from a slaty cleavage in the pelites towards a disjunctive cleavage in the more competent layers. Related fold styles are chevron to subsoclinal, with a decreasing apical angle towards the northern sectors (Section A-A'). The pelitic composition of the basal complex triggered disharmonic folding and enhanced shearing under the

same kinematic. Generally, folds show a constant asymmetry that suggests a tectonic transport towards SW, associated with a unique, progressive deformation (D1).

This is in agreement with the kinematic data from the genetically associated, underlying Penninic Basal Contact, where the Penninic wedge was translated from the hinterland towards the foreland [6,8,10,20,36]. This relatively simple fabric suddenly develops into more complex features, just across the bounding contact between of the Sanremo unit and the more internal flysch units or Briançonnais rocks. The internal Helminthoid Flysch nappes (Moglio–Testico, Borghetto, Colla Domenica–Leverone and Albenga) still show mainly SW-verging folds, but with markedly different fabric, characterized by abundant parasitic folds, folded veins, synthetic shear zones, crenulation cleavage and down-dip attitude (Figure 7b,c and Figure 8e,f). The recognition of some of these characteristics (i.e., a crenulation cleavage, folded veins and rare NE-ward fold asymmetry) have been commonly used as evidence of a second deformation phase (D2) superimposed onto the first one.

Nonetheless, most of the structures showing the deviating kinematic are strictly local, without any significant areal distribution. They are not associated with a foliation crosscutting an earlier one. These structures cannot be related to different kinematics, variation in the stress-field, nor to any change in metamorphic conditions. In fact, the stress orientation is generally an unknown parameter where strain is high; the fold orientation is largely controlled by the orientation of preexisting fabric and strain. Furthermore, local deviations of any sense of shear are more easily produced by wrench-components, rotation or pre-folding irregularities; finally a secondary cleavage commonly develops during progressive shearing in heterogeneous lithologies [4]. We must also stress that most of these structures show a regionally distributed top-to-SW sense of shear associated with coherent large folds. Therefore, there is no reason to invoke a different deformation phase to justify the presence of such complexities. Rather, the fold patterns depict noncylindrical geometries and the observed oblique fabrics suggest that noncoaxial progressive deformation [4] accumulated for some long time under a constant kinematic towards SW. We interpret the observed complex features as mainly being derived from the lithological and rheological heterogeneities related to the close alternation of competent and weak layers. Local variations of mechanical properties generate different responses to the imposed stress, and thus develop structures with different shapes and orientations.

On the contrary, the steeply dipping shear zones with both a top-to-NE and top-to-SW sense of shear that cross-cut the main folds (Figures 7c and 8f) are related to upright folds or high-angle shear zones that reshape the km-scale recumbent SW-verging nappes (Figures 4, 6 and 8). As the related fabric often displays different orientation, foliation and style, it has been grouped into a second foliation S2. This deformation fabric is furthermore associated with the steepening or overturning of the thrust surface between the Sanremo unit and the other Penninic units (Figures 4, 6 and 8). However, it should be noted that, in the field, S1- and S2-related fold asymmetry or overlapping foliations are difficult to discriminate, although in literature the SW- or NE-ward asymmetry has been widely used as the main criterion to discern between the two foliations, and consequently, between different deformation phases (D1 and D2). S2 fabric is bordered in the internal Flysch nappes and Briançonnais, whereas the Sanremo unit lacks any evidence of a different foliation. We further emphasize that, even in the internal part of the chain, clear S1–S2 occurrences are rare or ambiguous. Based on these considerations, we suggest that the S2 fabric was the result of the progressive evolution of the S1, which acquired different shapes in different domains of the orogen. Therefore, from a structural point of view, we cannot extrapolate a well-defined fabric characterizing a second deformation phase (D2) chronologically separated from the first one. No evidence of a third, ductile deformation phase has been found, neither as foliation nor as fold/fault structures.

In summary, the Sanremo unit experienced a different deformation history with respect to the other Helminthoid Flysch units, although they should share most of the translation path from the oceanic basin towards the Alpine wedge. In the following, we propose a kinematic model describing the emplacement of the Helminthoid Flysch in the Ligurian orogeny. The recognized deformation stages are then critically evaluated in relation to the geodynamic stages.

5.2. Kinematic Model

After their deposition in the Alpine Tethys oceanic environment [33–37], and as a consequence of the northward Adria movement, the Helminthoid Flysch, started to be incorporated into the accretionary prism in the uppermost Cretaceous–Paleocene (Figure 10a) ([7,9,36]. The Sanremo unit was the first to be accreted, as it occupied the innermost (southern) position. Micropaleontological data indicate an Early Eocene age for the turbidites of the Colla Domenica–Leverone and Albenga units [49,52]. As they were located at the transition between the oceanic realm and the European distal margin [9,19], this age constrains the involvement of all the Helminthoid Flysch nappes in the orogenic wedge since the Middle Eocene (Figure 10b). In these times, the oceanic basement and the internal portion of the Briançonnais experienced subduction-related deformation and metamorphism [6,13–16].

In the Late Eocene, high-pressure rocks were exhumed in the inner sector of the orogen (South), as constrained by thermochronometric dating and the Early Oligocene age of the post-collisional sediment of the Tertiary Piedmont Basin [18,56,57]. At this time, the Helminthoid Flysch nappes represented the orogenic lid, resting above the rest of the Penninic units. Contemporaneously, in the outer part of the growing orogenic chain, the Alpine Foreland Basin succession was deposited between the outermost Briançonnais and the Dauphinois domains [31,32,58,59]. The top of its siliciclastic turbidite sequence, the Flysch Noir, is characterized by the abundant olistostromes sourced from the Cretaceous carbonate turbidites of the Helminthoid Flysch [24,32,60]. The Late Priabonian–Early Oligocene age of this layer provides constraints for the arrival of the Sanremo unit, the emplacement of which marked the end of the deposition. Zircon (U-Th)/He dating between 34 and 28 Ma of the thrust activity [20] confirms that the Helminthoid Flysch bypassed—from south to north—the rest of the tectonic pile during the Late Eocene. This would suggest that, by this time, the flysch units accomplished the reversal of their original paleogeographic setting. In particular, the innermost Sanremo unit was translated towards the outermost position. In order to fit such a timing and geometry, four out-of-sequence thrusting steps (progressively younger from north to south) must be introduced (Figure 10c,d). This kinematic produced the foreland-dipping nappes that characterize the internal Flysch units, as well as the Arnasco–Castelbianco Pre-piedmont unit [55]. The preserved small fragments of the normal limb of this last unit could derive from an enhanced shearing of the flysch units translating above it. Overall, the km-scale, SW-verging and -plunging recumbent folds of the Helminthoid Flysch associated with the S1 formed during this subduction-related geodynamic setting (D1 [6,8,10,53]).

In the Early Oligocene times, the subduction dynamic turns towards collision between Adria and Europe. Furthermore, the motion vector of the Adriatic microplate (with respect to Europe) changed from northward to northwest-ward [61,62]. In the Western Alps that comprise the Ligurian segment, the indentation of the Ivrea body generates backfolding and backthrusting in the inner zone of the orogeny (e.g., [5–8,62,63]). In the area examined in this work, however, the associate D2 deformation features are weak and restricted to the internal flysch units, whereas the Sanremo nappe seems to have escaped this deformation. As the Sanremo unit was already emplaced in the outer sector of the chain, the frontal flexure of the European plate continued to migrate northwestward in Early-Late Oligocene times as recorded by the migrating Alpine Foreland Basin (Figure 10e). The inner orogeny instead experienced a thickening of the orogenic wedge and the development of substantial topographic relief which represented the source area of the retro-foreland Tertiary Piedmont Basin. This collision-related geodynamic setting (D2 [6,8,10,53]) justifies the compartmentalization of the deformation. The reshaping of the SW-plunging structure by S2-related upright folds and sub-vertical shear zones developed above the deep collision between the Ivrea body and the European basement (internal zones), whereas the foreland records only the outward propagation of the deformation.

Since the Late Oligocene, the transtensional regime was generated ahead of the apical closure of the Liguro–Provençal rifting, connecting the opposite movements of the Alpine and Apennines arcs. Since the Early Miocene, the oceanic spreading of the Liguro–Provençal and Tyrrhenian basins produced the counterclockwise rotation of the Ligurian segment and the Corsica–Sardinia drifting [28,29].

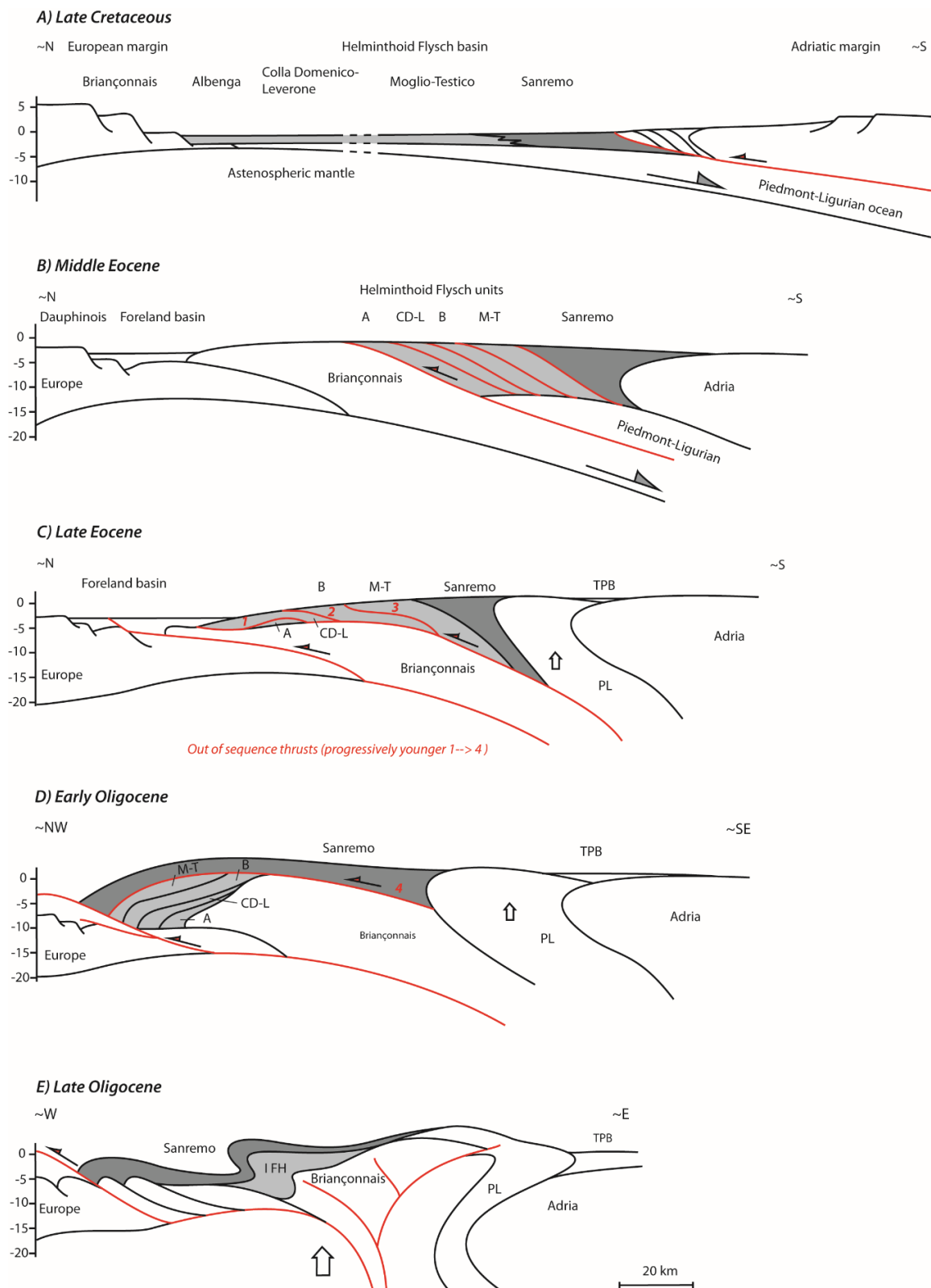


Figure 10. Geodynamic sketch showing the kinematic path of the Helminthoid Flysch nappes within the evolution of the Ligurian orogen between the Cretaceous–Oligocene times, after [8]. TPB: Tertiary Piedmont Basin.

6. Conclusions

Field-based structural investigations of the Helminthoid Flysch nappes of the Ligurian Alps reveal important strain partitioning at the orogeny scale. Heterogeneous fabrics characterize units that share the same paleogeographic provenance and similar lithostratigraphy derived from the common pre-collisional flysch-type sedimentation in the Alpine Tethys oceanic environment. However, correlations among different cross-sections expose contrasting deformation patterns between the topmost and outermost nappe (the Sanremo unit) and the rest of the flysch units (Moglio–Testico, Borghetto, Colla Domenica–Leverone and Albenga). The traditional description of the Alpine deformation through three phases is critically evaluated and reinterpreted based on field evidences and regional correlations. Spatial and temporal variations of the deformation features allow the introduction of a kinematic model that justifies the present-day position of the Helminthoid Flysch nappe in the outermost part of the chain.

Author Contributions: Conceptualization, M.M.; Data curation, P.M. and S.S.; Funding acquisition, S.S.; Investigation, P.M., M.M. and S.S.; Methodology, P.M.; Supervision, S.S.; Writing—original draft, P.M. and M.M.; Writing—review & editing, M.M. All authors have read and agreed to the published version of the manuscript.

Funding: This research received no external funding.

Acknowledgments: We are grateful to journal editor Annie Zhou and the anonymous reviewers for significantly improving the clarity of our manuscript and helpful comments.

Conflicts of Interest: The authors declare no conflicts of interest.

References

1. Ramsay, J.G. *Folding and Fracturing of Rocks*; McGraw-Hill: New York, NY, USA, 1967.
2. Park, R.G. Structural correlation in metamorphic belts. *Tectonophysics* **1969**, *7*, 323–338. [[CrossRef](#)]
3. Passchier, C.W.; Trouw, R.A.J. *Microtectonics*, 2nd ed.; Springer: Berlin, Germany, 2005.
4. Fossen, H.; Cavalcante, G.C.G.; Pinheiro, R.V.L.; Archanjo, C.J. Deformation—Progressive or multiphase? *J. Struct. Geol.* **2019**, *125*, 82–99. [[CrossRef](#)]
5. Trümpy, R. Paleotectonic evolution of the central and western Alps. *GSA Bull.* **1960**, *71*, 843–907. [[CrossRef](#)]
6. Vanossi, M.; Cortesogno, L.; Galbiati, B.; Messiga, B.; Piccardo, G.B.; Vannucci, R. Geologia delle Alpi Liguri: Dati, problemi, ipotesi. *Mem. Soc. Geol. Ital.* **1986**, *28*, 5–75.
7. Dal Piaz, G.V.; Bistacchi, A.; Massironi, M. Geological outline of the Alps. *Episodes* **2003**, *26*, 175–180. [[CrossRef](#)] [[PubMed](#)]
8. Bonini, L.; Dallagiovanna, G.; Seno, S. The role of pre-existing faults in the structural evolution of thrust systems: Insights from the Ligurian Alps (Italy). *Tectonophysics* **2010**, *480*, 73–87. [[CrossRef](#)]
9. Decarlis, A.; Dallagiovanna, G.; Lualdi, A.; Maino, M.; Seno, S. Stratigraphic evolution in the Ligurian Alps between Variscan heritages and the Alpine Tethys opening: A review. *Earth Sci. Rev.* **2013**, *125*, 43–68. [[CrossRef](#)]
10. Seno, S.; Dallagiovanna, G.; Vanossi, M. A kinematic evolution model for the Penninic sector of the central Ligurian Alps. *Int. J. Earth Sci.* **2005**, *94*, 114–129. [[CrossRef](#)]
11. Piccardo, G.B. Le ofioliti metamorfiche del Gruppo di Voltri, Alpi Liguri: Caratteri primari ed interpretazione geodinamica. *Mem. Soc. Geol. Ital.* **1984**, *28*, 95–114.
12. Lemoine, M.; Bas, T.; Arnaud-Vanneau, A.; Arnaud, H.; Dumont, T.; Gidon, M.; Bourbon, M.; de Graciansky, P.-C.; Rudkiewicz, J.-L.; Tricart, P. The continental margin of the mesozoic tethys in the western Alps. *Mar. Pet. Geol.* **1986**, *3*, 179–199. [[CrossRef](#)]
13. Messiga, B. Alpine metamorphic evolution of Ligurian Alps (North-West Italy): Chemography and petrological constraints inferred from metamorphic climax assemblages. *Contrib. Mineral. Petrol.* **1987**, *95*, 269–277. [[CrossRef](#)]
14. Messiga, B.; Oxilia, M.; Piccardo, G.B.; Vanossi, M. Fasi metamorfiche e deformazioni Alpine nel Brianzese e nel Pre-Piemontese-Piemontese esterno delle Alpi Liguri: Un possibile modello evolutivo. *Rend. Soc. Ital. Mineral. Petrol.* **1981**, *38*, 261–280.

15. Desmons, J.; Aprahamian, J.; Compagnoni, R.; Cortesogno, L.; Frey, M.; Gaggero, L.; Seno, S. Alpine metamorphism of the western Alps: I. Middle to high T/P metamorphism. *Schweiz. Mineral. Petrogr. Mitt.* **1999**, *79*, 89–110.
16. Federico, L.; Crispini, L.; Scambelluri, M.; Capponi, G. Ophiolite mélangé zone records exhumation in a fossil subduction channel. *Geology* **2007**, *35*, 499–502. [[CrossRef](#)]
17. Bonazzi, A.; Cobiانchi, M.; Galbiati, B. Primi dati sulla cristallinità dell'illite nelle unità tettoniche più esterne e strutturalmente più elevate delle Alpi Liguri. *Atti Tic. Sci. Terra* **1988**, *31*, 63–77.
18. Maino, M.; Dallagiovanna, G.; Dobson, K.J.; Gaggero, L.; Persano, C.; Seno, S.; Stuart, F.M. Testing models of orogen exhumation using zircon (U-Th)/He thermochronology: Insight from the Ligurian Alps, Northern Italy. *Tectonophysics* **2012**, *560–561*, 84–93. [[CrossRef](#)]
19. Decarlis, A.; Fellin, M.G.; Maino, M.; Ferrando, S.; Manatschal, G.; Gaggero, L.; Seno, S.; Stuart, F.M.; Beltrando, M. Tectono-thermal Evolution of a Distal Rifted Margin: Constraints from the Calizzano Massif (Prepiedmont-Briançonnais Domain, Ligurian Alps). *Tectonics* **2017**, *36*, 3209–3228. [[CrossRef](#)]
20. Maino, M.; Casini, L.; Ceriani, A.; Decarlis, A.; Di Giulio, A.; Seno, S.; Setti, M.; Stuart, F.M. Dating shallow thrusts with zircon (U-Th)/He thermochronometry—The shear heating connection. *Geology* **2015**, *43*, 495–498. [[CrossRef](#)]
21. Carminati, E.; Gosso, G. Structural map of a Ligurian Briançonnais cover nappe (Conca delle Carsene, Monte Marguareis, Ligurian Alps, Italy) and explanatory notes. *Mem. Soc. Geol.* **2000**, *52*, 93–99.
22. Maino, M.; Bonini, L.; Dallagiovanna, G.; Seno, S. Large sheath folds in the Briançonnais of the Ligurian Alps reconstructed by analysis of minor structures and stratigraphic mapping. *J. Maps* **2015**, *11*, 157–167. [[CrossRef](#)]
23. Ceriani, S.; Fugenschuh, B.; Schmid, S.M. Multi-stage thrusting at the “Penninic Front” in the Western Alps between Mont Blanc and Pelvoux massifs. *Int. J. Earth Sci.* **2001**, *90*, 685–702. [[CrossRef](#)]
24. Maino, M.; Seno, S. The thrust zone of the Ligurian Penninic basal contact (Monte Frontè, Ligurian Alps, Italy). *J. Maps* **2016**, *12*, 341–351. [[CrossRef](#)]
25. Capponi, G.; Crispini, L. Structural and metamorphic signature of alpine tectonics in the Voltri Massif (Ligurian Alps, North-Western Italy). *Eclogae Geol. Helv.* **2002**, *95*, 31–42.
26. Alvarez, W.; Coccozza, T.; Wezel, F.C. Fragmentation of Alpine orogenic belt by microplate dispersal. *Nature* **1974**, *248*, 309–314. [[CrossRef](#)]
27. Rosenbaum, G.; Lister, G.S.; Duboz, C. Relative motion of Africa, Iberia and Europe during the Alpine orogeny. *Tectonophysics* **2002**, *359*, 117–129. [[CrossRef](#)]
28. Maffione, M.; Speranza, F.; Faccenna, C.; Cascella, A.; Vignaroli, G.; Sagnotti, L. A synchronous Alpine and Corsica–Sardinia rotation. *J. Geophys. Res.* **2008**, *113*, B03104. [[CrossRef](#)]
29. Maino, M.; Decarlis, A.; Felletti, F.; Seno, S. Tectono-sedimentary evolution of the tertiary piedmont basin (NW Italy) within the Oligo-Miocene central Mediterranean geodynamics. *Tectonics* **2013**, *32*, 593–619. [[CrossRef](#)]
30. Federico, L.; Crispini, L.; Vigo, A.; Capponi, G. Unravelling polyphase brittle tectonics through multi-software fault-slip analysis: The case of the Voltri Unit, Western Alps (Italy). *J. Struct. Geol.* **2014**, *68*, 175–193. [[CrossRef](#)]
31. Decarlis, A.; Maino, M.; Dallagiovanna, G.; Lualdi, A.; Masini, E.; Seno, S. Salt tectonics in the SW Alps (Italy-France): From rifting to the inversion of the European continental margin in a context of oblique convergence. *Tectonophysics* **2014**, *636*, 293–314. [[CrossRef](#)]
32. Lanteaume, M. Considerations paléogéographiques sur la patrie supposée de la nappe du flysch ad Helminthoïdes et al liason Alpen-Apennins. *Livre Mém. Profr. Paul Fallot* **1962**, *2*, 257–272.
33. Galbiati, B. L'unità di Borghetto ed i suoi legami con quella di Moglio-Testico (Alpi Liguri): Conseguenze paleogeografiche. *Riv. Ital. Paleontol. Stratigr.* **1984**, *90*, 205–226.
34. Sagri, M. Litologia, stratimetria e sedimentologia delle torbiditi di piana di bacino del Flysch di San Remo (Cretaceo superiore, Liguria occidentale). *Mem. Soc. Geol. Ital.* **1984**, *28*, 577–586.
35. Di Giulio, A. Structural evolution of S.Remo and Moglio-Testico units (Piemontese-Ligurian Flysch, Maritime Alps): Abstract. *Rend. Soc. Geol. Ital.* **1988**, *11*, 61–64.
36. Di Giulio, A. The evolution of the Western Ligurian Flysch Units and the role of mud diapirism in ancient accretionary prisms (Maritime Alps, Northwestern Italy). *Int. J. Earth Sci. (Geol. Rundsch.)* **1992**, *81*, 655–668. [[CrossRef](#)]

37. Mueller, P.; Patacci, M.; Di Giulio, A. Hybrid event beds in the proximal to distal extensive lobe domain of the coarse-grained and sand-rich Bordighera turbidite system (NW Italy). *Mar. Pet. Geol.* **2017**, *86*, 908–931. [[CrossRef](#)]
38. Mueller, P.; Langone, A.; Patacci, M.; Di Giulio, A. Detrital signatures of impending collision: The deep-water record of the Upper Cretaceous Bordighera Sandstone and its basal complex (Ligurian Alps, Italy). *Sediment. Geol.* **2018**, *377*, 147–161. [[CrossRef](#)]
39. Mueller, P.; Langone, A.; Patacci, M.; Di Giulio, A. Towards a southern European Tethyan palaeomargin provenance signature: Sandstone detrital modes and detrital zircon U-Pb age distribution of the upper cretaceous—Paleocene monte bignone sandstones (Ligurian Alps, NW Italy). *Int. J. Earth Sci.* **2019**. [[CrossRef](#)]
40. Lanteaume, M. Contribution à l'étude géologique des Alpes Maritimes Franco-Italiennes. Stratigraphie des Unités Briançonnaises (Unités du Massif du Marguareis, du Monte Armetta, de Poggio Castelvevchio et des Schistes grésocalcaires). *Mèm. Serv. Cart. Géol. Fr. (Et Cnrs)* **1968**, 405. Available online: <https://tel.archives-ouvertes.fr/tel-00802328> (accessed on 11 January 2020).
41. Lanteaume, M.; Radulescu, N.; Gavos, M.; Feraud, J. *Notice Explicative, Carte Géol. De France (1/50.000), Feuille Viève-Tende (948)*; BRGM: Orleans, France, 1990; p. 139.
42. Casini, L.; Cuccuru, S.; Maino, M.; Oggiano, G.; Tiepolo, M. Emplacement of the Arzachena Pluton (Corsica–Sardinia Batholith) and the geodynamics of incoming Pangaea. *Tectonophysics* **2012**, *544*, 31–49. [[CrossRef](#)]
43. Casini, L.; Cuccuru, S.; Maino, M.; Oggiano, G.; Puccini, A.; Rossi, P. Structural map of Variscan northern Sardinia (Italy). *J. Maps* **2015**, *11*, 75–84. [[CrossRef](#)]
44. Dallagiovanna, G.; Gaggero, L.; Maino, M.; Seno, S.; Tiepolo, M. U-Pb zircon ages for post-Variscan volcanism in the Ligurian Alps (Northern Italy). *J. Geol. Soc. Lond.* **2009**, *166*, 101–114. [[CrossRef](#)]
45. Maino, M.; Dallagiovanna, G.; Gaggero, L.; Seno, S.; Tiepolo, M. U-Pb zircon geochronological and petrographic constraints on late to post-collisional Variscan magmatism and metamorphism in the Ligurian Alps, Italy. *Geol. J.* **2012**, *47*, 632–652. [[CrossRef](#)]
46. Maino, M.; Gaggero, L.; Langone, A.; Seno, S.; Fanning, M. Cambro-Silurian magmatism at the northern Gondwana margin (Penninic basement of the Ligurian Alps). *Geosci. Front.* **2019**, *10*, 315–330. [[CrossRef](#)]
47. Decarlis, A.; Lualdi, A. Synrift sedimentation on the northern Tethys margin: An example from the Ligurian Alps (Upper Triassic to Lower Cretaceous, Prepidmont domain, Italy). *Int. J. Earth Sci.* **2011**, *100*, 1589–1604. [[CrossRef](#)]
48. Cardozo, N.; Allmendinger, R.W. Stereonet3D. 2011. Available online: [http://www.ux.uis.no/\\$\sim\\$nestor/work/programs.html](http://www.ux.uis.no/\simnestor/work/programs.html) (accessed on 10 January 2020).
49. Cobianchi, M.; Di Giulio, A.; Galbiati, B.; Mosna, S., II. “Complesso di base” del Flysch di San Remo nell'area di San Bartolomeo, Liguria occidentale (nota preliminare). *Atti Ticinesi Sci. Terra* **1991**, *34*, 145–154.
50. Kerckhove, C. La “zone du Flysch” dans les nappes de l'Embrunais-Ubaye (Alpes occidentales). *Geol. Alps* **1969**, *45*, 5–204.
51. Brizio, D.; Deregibus, C.; Eusebio, A.; Gallo, M.; Gosso, G.; Rattalino, E.R.F.; Tosetto, S.; Oxilia, M. Guida all'escursione: I rapporti tra la zona Brianzonese Ligure e il Flysch a Elmintoidi, Massiccio del Marguareis (Limone Piemonte–Certosa di Pesio, Cuneo, 14/15 Settembre 1983). *Mem. Soc. Geol.* **1983**, *26*, 579–595.
52. Vanossi, M. *Guide Geologiche Regionali: Alpi Liguri*; BE-MA Editrice S.R.L.: Milano, Italy, 1991; p. 295.
53. Vanossi, M.; Gosso, G. Introduzione alla geologia del Brianzonese Ligure. *Mem. Soc. Geol. Ital.* **1983**, *26*, 441–461.
54. Seno, S.; Dallagiovanna, G.; Maino, M.; Decarlis, A.; Bonini, L.; Toscani, G.; Pellegrini, L. Foglio 259 Imperia. Carta Geol. D'italia Alla Scala 1:50,000. Serv. Geol. D'italia. Roma. 2012. Available online: http://www.isprambiente.gov.it/Media/carg/259_IMPERIA/Foglio.html (accessed on 10 January 2020).
55. Dallagiovanna, G.; Seno, S. Rilevamento geologico ed analisi strutturale del settore meridionale dell'unità di Arnasco-Castelbianco (Alpi Marittime). *Mem. Soc. Geol. Ital.* **1984**, *28*, 441–445.
56. Gelati, R.; Gnaccolini, M. Synsedimentary tectonics and sedimentation in the Tertiary Piedmont Basin, Northwestern Italy. *Riv. Ital. Paleontol. Stratigr.* **1998**, *104*, 193–214.
57. Federico, L.; Capponi, G.; Crispini, L.; Scambelluri, M.; Villa, I.M. ³⁹Ar/⁴⁰Ar dating of high-pressure rocks from the Ligurian Alps: Evidence for a continuous subduction-exhumation cycle. *Earth Planet. Sci. Lett.* **2005**, *240*, 668–680. [[CrossRef](#)]

58. Sinclair, H.D. Tectonostratigraphic model for underfilled peripheral foreland basins: An Alpine perspective. *GSA Bull.* **1997**, *109*, 324–346. [[CrossRef](#)]
59. Ford, M.; Lickorisch, W.H.; Kuszniir, N.J. Tertiary foreland sedimentation in the southern subalpine chains, SE France: Geodynamic appraisal. *Basin Res.* **1999**, *11*, 315–336. [[CrossRef](#)]
60. Perotti, E.; Bertok, C.; D’Atri, A.; Martire, L.; Piana, F.; Catanzariti, R. A tectonically-induced Eocene sedimentary mélangé in the West Ligurian Alps, Italy. *Tectonophysics* **2012**, *568–569*, 200–214. [[CrossRef](#)]
61. Dewey, J.F.; Helman, M.L.; Knott, S.D.; Turco, E.; Hutton, D.H.W. Kinematics of the western Mediterranean. *Geol. Soc. Lond. Spec. Publ.* **1989**, *45*, 265–283. [[CrossRef](#)]
62. Schmid, S.M.; Pfiffner, O.A.; Froitzheim, N.; Schonborn, G.; Kissling, E. Geophysical-geological transect and tectonic evolution of the Swiss-Italian Alps. *Tectonics* **1996**, *15*, 1036–1064. [[CrossRef](#)]
63. Ford, M.; Duchene, S.; Gasquet, D.; Vanderhaeghe, O. Two-phase orogenic convergence in the external and internal SW Alps. *J. Geol. Soc.* **2006**, *163*, 815–826. [[CrossRef](#)]



© 2020 by the authors. Licensee MDPI, Basel, Switzerland. This article is an open access article distributed under the terms and conditions of the Creative Commons Attribution (CC BY) license (<http://creativecommons.org/licenses/by/4.0/>).